

Thermophysical properties of Sander sandstone using Transient Hot-Bridge sensor



Muhammad Abid

Physikalisch-Technische Bundesanstalt (PTB),
Braunschweig

Objectives

- Characterization of Sander sandstone
- Prediction of thermal properties using THB sensor
- Effect of various fluids on thermal performance
- Comparison of experimental results with various existing mixing and empirical laws
- Proposing an empirical relation to predict effective thermal conductivity

1. Characterization of Sander sandstone

- Density and porosity

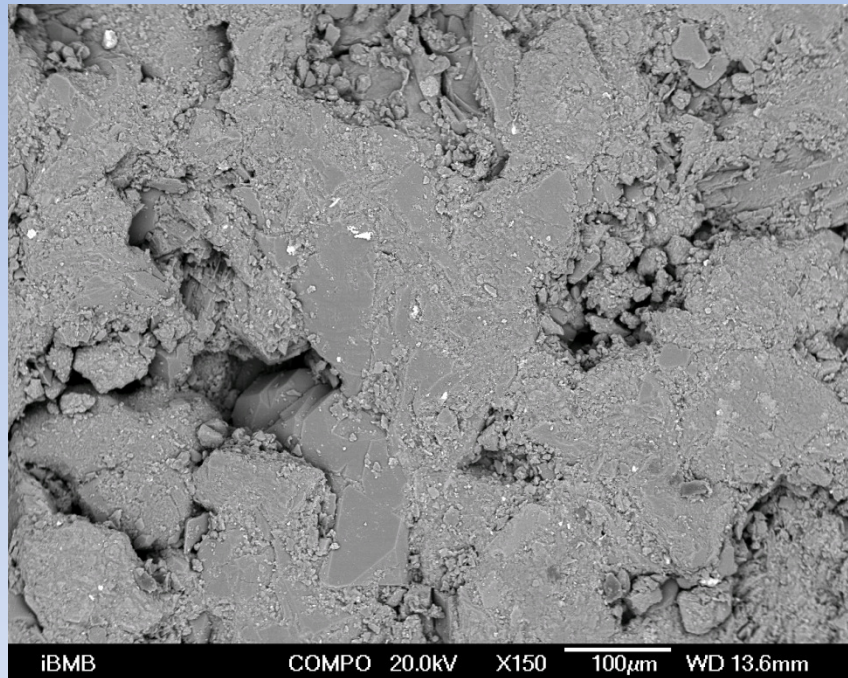
Bulk density (kgm^{-3})		Water porosity (%)		
Dry	Water-saturated	Calculated	Calculated by MIP	Published [3]
2081	2247	16.54	18.62	17.80

- Thermophysical properties of mineral components

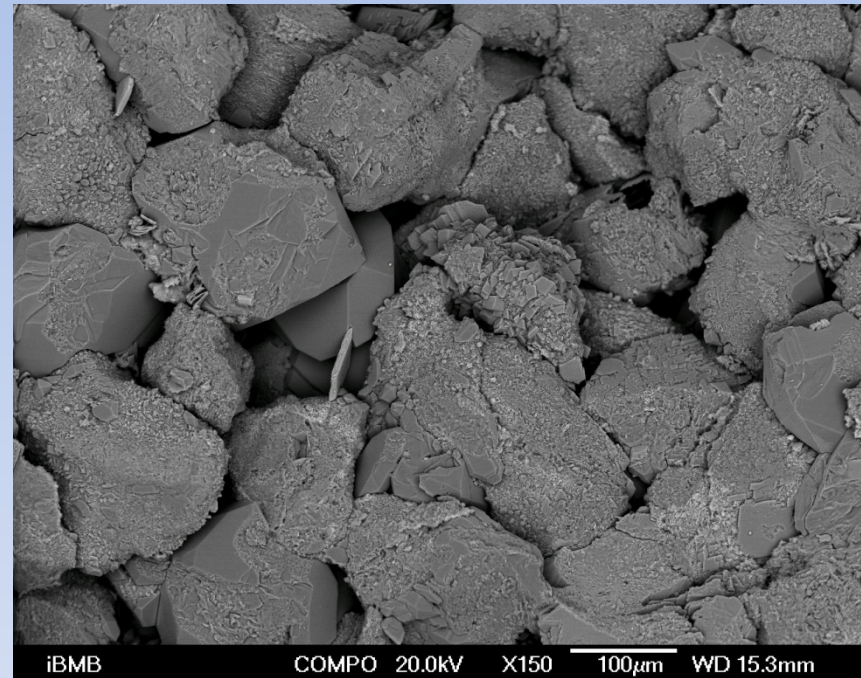
Parameters	Mineral components			
	Quartz	Feldspar	Mica	Plagioclase
Volume fraction (%)	54	21	18	7
Thermal conductivity ($\text{Wm}^{-1}\text{K}^{-1}$) [1]	4.52 ^a	2.31	2.28	2.09
Thermal diffusivity (mm^2s^{-1})	2.31	1.31	1.05	1.09
Specific heat capacity ($\text{Jkg}^{-1}\text{K}^{-1}$) [2]	740	685	760	730
Density (kgm^{-3}) [1,2]	2648	2590	2850	2620

^[a] Average value of α -quartz and fused quartz has been taken.

SEM Images

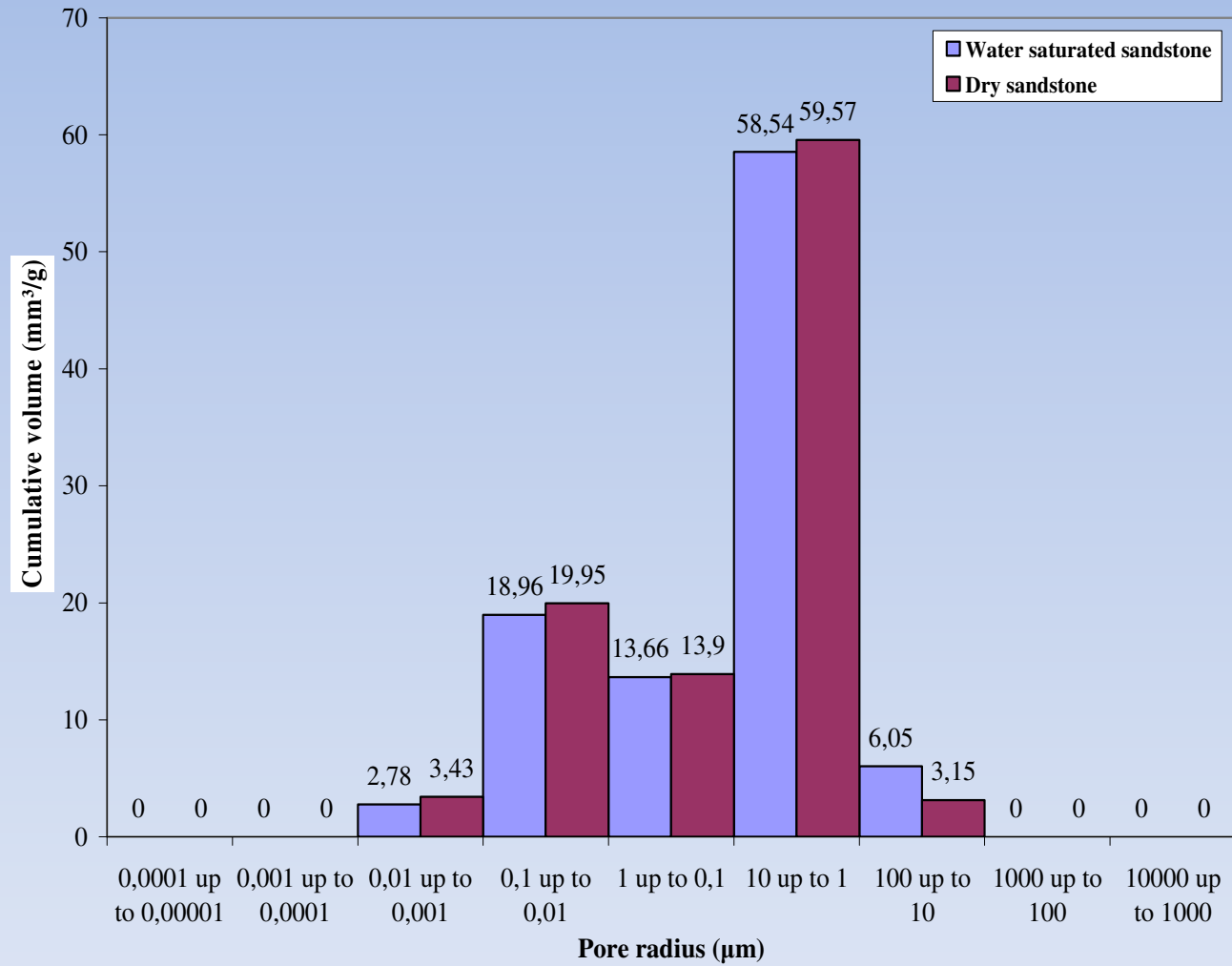


- Surface image



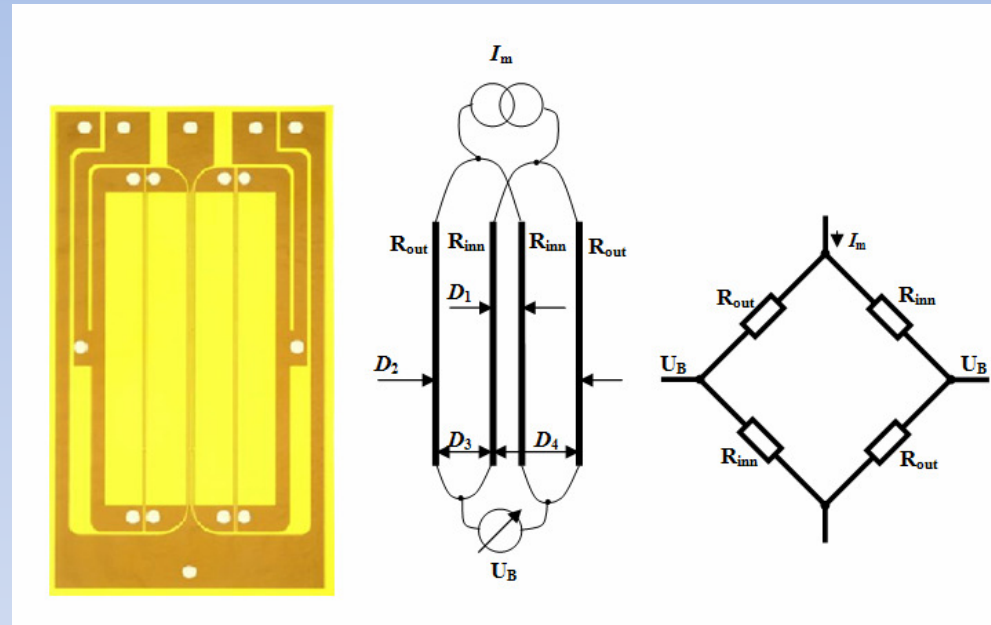
- Inside image

Pore size distribution using MIP



2. Features of Transient Hot-bridge sensor

- Transient Hot Bridge (THB) is a highly sensitive thermoelectric sensor
- Rapid thermal conductivity and diffusivity measurements
- Ability to measure from 0.02 to 100 W/mK at temperatures up to 250 °C
- Three thermophysical parameters in one single experiment



2.1. Working equation for THB sensor

- The general equation for thermal conductivity measurement with THB sensor is,

$$\lambda = 0.98 \frac{\alpha R_{eff}^2}{4\pi L_{eff} m} \left(\frac{I_S}{2} \right)^3 \quad \dots\dots\dots 1$$

$$C_p = \frac{\lambda}{a\rho} \quad \dots\dots\dots 2$$

Where, α is the temperature coefficient of resistance

R_{eff} is the effective resistance of the sensor

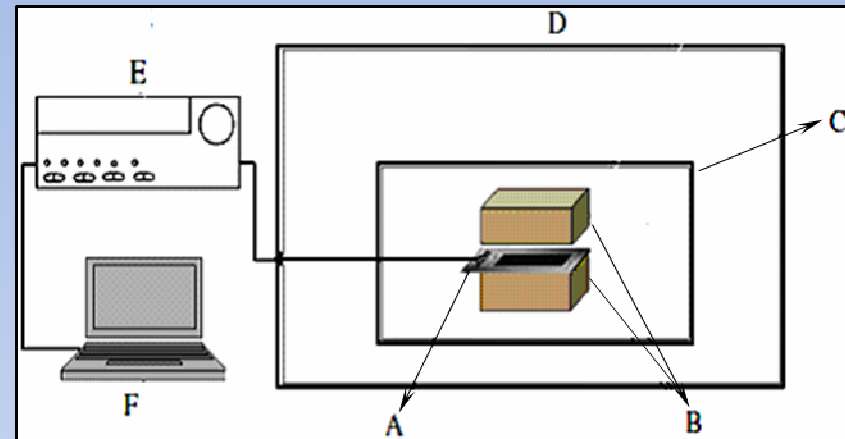
L_{eff} is the effective length of the sensor

I_S is the electrical current through THB-Sensor

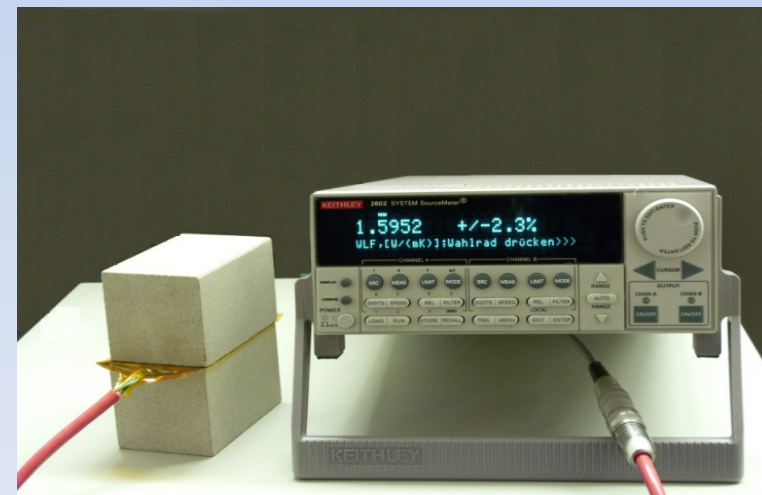
and $m = \frac{U_2 - U_1}{\ln(t_2 / t_1)}$ slope of the THB-signal

3. Experimental setup

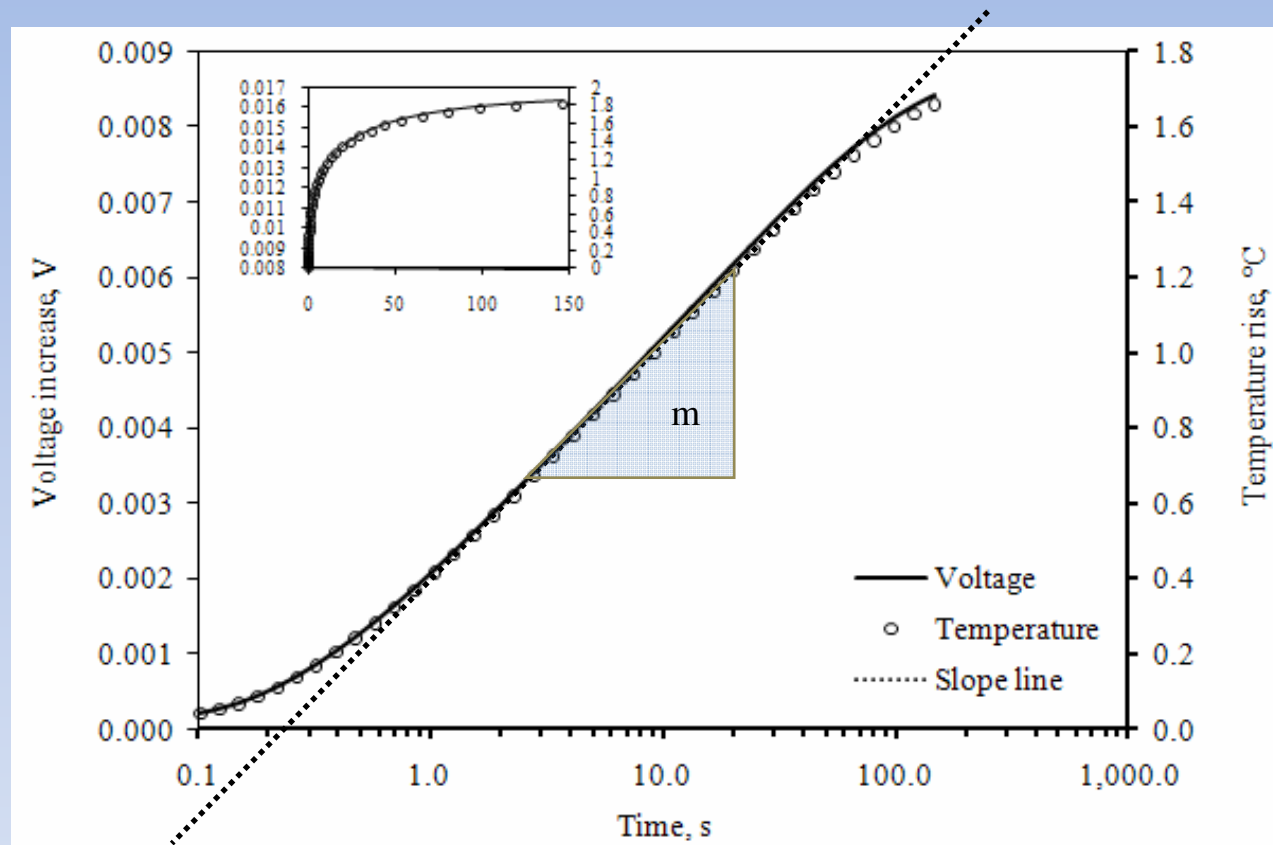
- Sample dimensions are $60 \times 60 \times 100 \text{ mm}^3$ each
- A programmable current source
- Output Signal is obtained in the form of voltage as a function of time
- Thermal conductivity and diffusivity are then calculated from the slope of the output signal



(A) THB sensor, (B) sample halves, (C) air-tight box, (D) climate chamber, (E) Keithley 2602 programmable source meter, (F) computer.

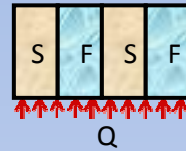


$$\lambda = 0.98 \frac{\alpha R_{eff}^2}{4\pi L_{eff} m} \left(\frac{I_s}{2} \right)^3$$



4. Theoretical models to predict λ

- Parallel model $\lambda_e^P = \phi\lambda_f + \lambda_s(1-\phi)$



- Series model $\lambda_e^S = \left[\frac{\phi}{\lambda_f} + \frac{(1-\phi)}{\lambda_s} \right]^{-1}$



- Horai model $\lambda_e^H = \left(\frac{\lambda_e^S + \lambda_e^P}{2} \right)$

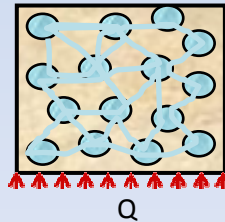
- Maxwell-Eucken upper model

$$\lambda_e^{MEU} = \lambda_f \frac{3 + 2(1-\phi)\left(\frac{\lambda_s}{\lambda_f} - 1\right)}{3 + (1-\phi)\left(\frac{\lambda_f}{\lambda_s} - 1\right)}$$

- Maxwell-Eucken lower model

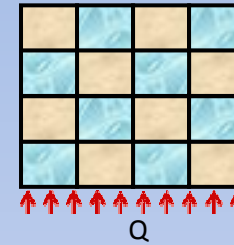
$$\lambda_e^{MEL} = \lambda_s \frac{3 + 2\phi\left(\frac{\lambda_f}{\lambda_s} - 1\right)}{3 + \phi\left(\frac{\lambda_s}{\lambda_f} - 1\right)}$$

- Assad's model $\lambda_e^A = \lambda_s \left(\frac{\lambda_f}{\lambda_s} \right)^m$

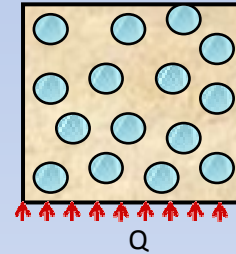


- Effective mean theory

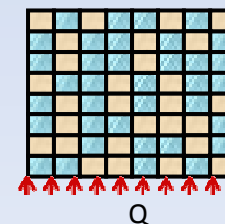
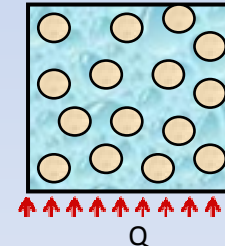
$$\lambda_e^{EMT} = 0.25 \left[(3\phi - 1)\lambda_f + (3(1-\phi) - 1)\lambda_s + \sqrt{\left((3\phi - 1)\lambda_f + (3(1-\phi) - 1)\lambda_s \right)^2 + 8\lambda_s\lambda_f} \right]$$



$$\lambda_{cont} > \lambda_{disp}$$



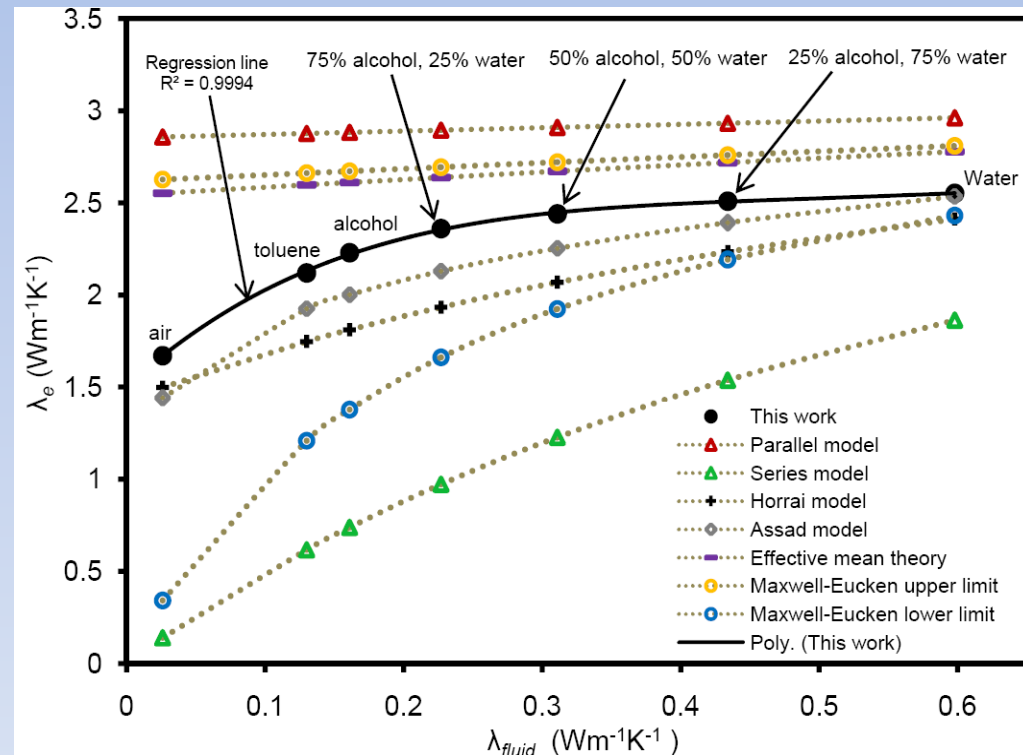
$$\lambda_{cont} < \lambda_{disp}$$



5. Experimental results

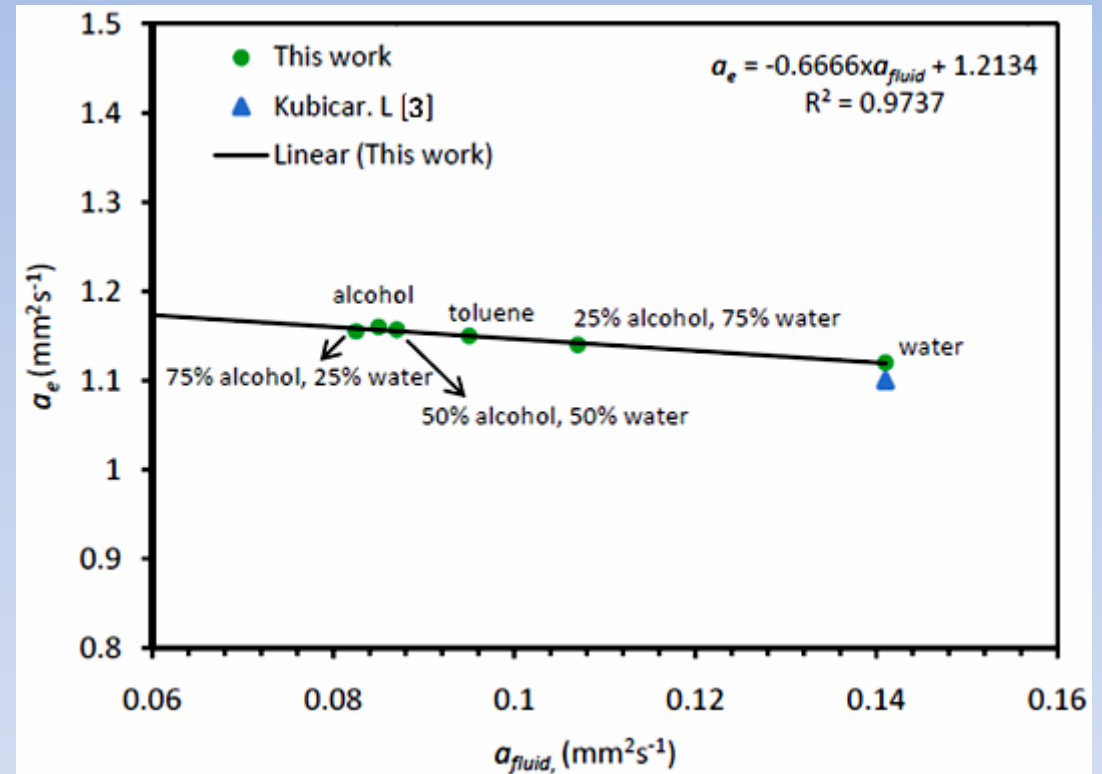
5.1. Thermal conductivity

- λ_e of Sander sandstone increases nonlinearly by increasing the λ_{fluid}
- Results of those models which take into account the structural characteristics are more closer to our experimental values
- Maximum error in case of Assad's model is $\pm 15\%$
- Difference decreases as the value of $\lambda_e/\lambda_{fluid}$ decreases



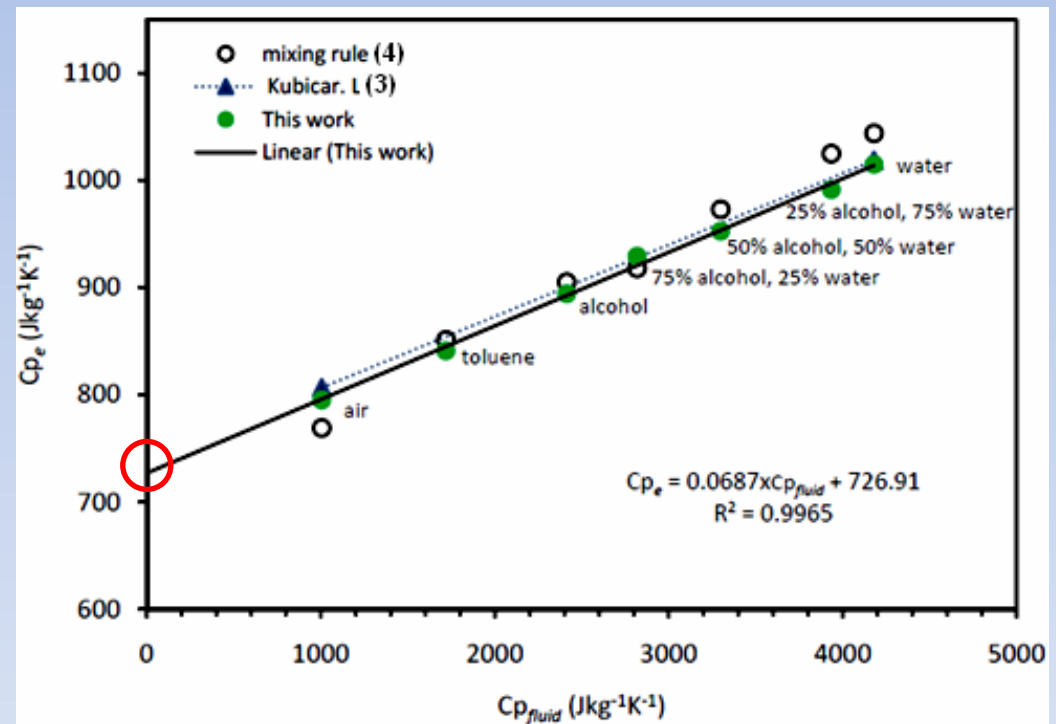
5.2. Thermal diffusivity

- Linear dependence
- A small change of about 5% (ranging from 1.11 to 1.17 mm^2s^{-1}) for all saturation cases



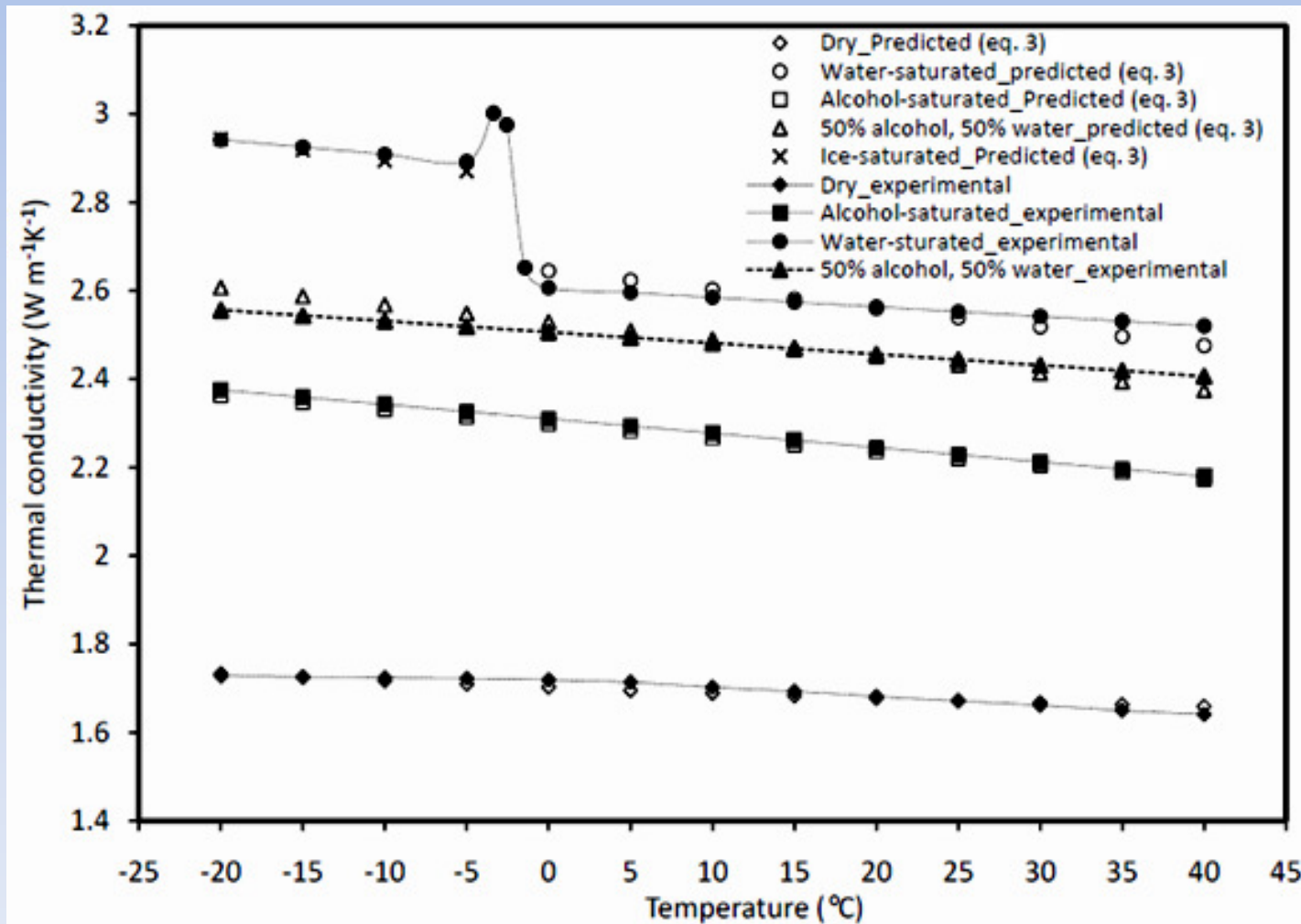
5.3. Specific heat capacity

- Linear dependence
- Intersection at y-axis gives the average specific heat capacity of the solid constituents ($Cp_{solid} = 728.75 \text{ Jkg}^{-1}\text{K}^{-1}$)



6. Developing a general equation for $\lambda(T)$

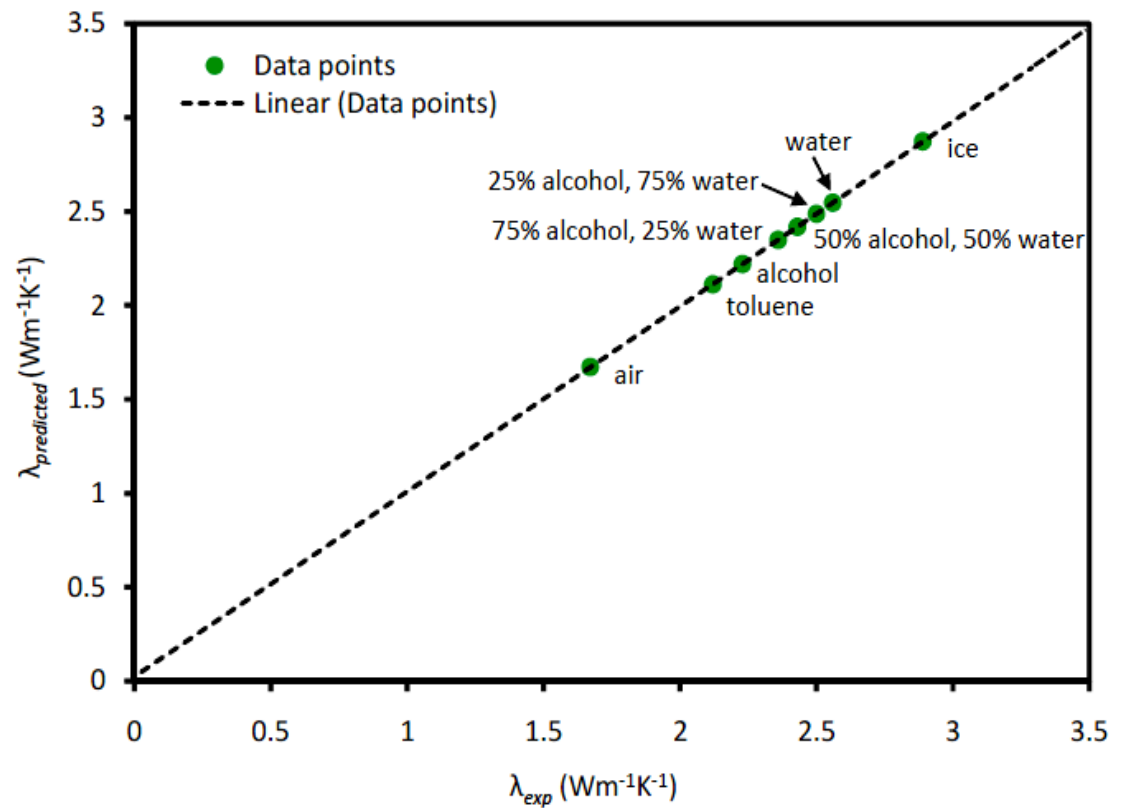
$$\lambda_{eff} = \left(\frac{(1.08\lambda_{25} - 0.15)^2}{\lambda_{25}(1.09 + 0.0033T) - 0.009T - 0.149} \right) - 0.0048T + 0.065 \quad \dots\dots\dots 3$$



7. Result comparision at 25 °C

Saturating fluid	Error ($\Delta\lambda^b$) in percent
Air (dry sandstone)	$-1.10 \leq \Delta\lambda \leq 1.09$
Alcohol	$0.30 \leq \Delta\lambda \leq 0.51$
50% alcohol, 50% water	$-1.99 \leq \Delta\lambda \leq 1.33$
Water	$-1.45 \leq \Delta\lambda \leq 1.80$
Ice	$-0.06 \leq \Delta\lambda \leq 0.76$

$$^b\Delta\lambda = [(\lambda_{exp} - \lambda_{fit}) / \lambda_{fit}] \times 100$$



Conclusions

- λ_{eff} of Sander sandstone increases nonlinearly by increasing the thermal conductivity of pore filling fluids
- Results of those models which take into account the structural characteristics are more closer to our experimental values
- the specific heat capacity of Sander sandstone increases linearly by increasing the specific heat capacity of pore filling fluids
- Negligible effect on thermal diffusivity
- An empirical relation has been proposed to calculate effective thermal conductivity of sandstone filled with different saturates
- λ_{eff} of Sander sandstone is directly proportional to λ_{25} and inversely proportional to the temperature (T)
- Transient hot-bridge sensor is an excellent sensor to measure thermophysical properties of porous rocks like sandstone

Thank you

References

- [1] Horai K and Simmons G 1969 *Earth and Planet. Sci. Lett.* **6** 359-368
- [2] Douglas W and Jacob S 2004 *Natural Resources Research* **13** 97-22
- [3] Kubicar L, Vretenar V, Bohac V and Tiano P 2006 *Int. J. Thermophys.* **27** 220-34
- [4] Douglas W and Jacob S 2004 *Natural Resources Research* **13** 123-130

Mixing rule for specific heat capacity

$$Cp_e = \left[\frac{\rho_{solid} Cp_{solid} (1-\phi) + \rho_{fluid} Cp_{fluid} \phi}{\rho_e} \right]$$

Table

Pore filling fluid	λ_{solid} ($Wm^{-1}K^{-1}$) [15,16]	λ_{exp} ($Wm^{-1}K^{-1}$)	a_{solid} (mm^2s^{-1}) [15,22]	a_{exp} (mm^2s^{-1})	a_e (mm^2s^{-1}) [7]	Cp_{solid} ($Jkg^{-1}K^{-1}$) [15,23]	Cp_{exp} ($Jkg^{-1}K^{-1}$)	Cp_e ($Jkg^{-1}K^{-1}$) [7]	Cp_e ($Jkg^{-1}K^{-1}$) [eq. 10]	ρ_{eff} (kgm^{-3})
Air	0.026	1.67	18.50	1.010	1.035	1005	795	806	769	2081
Toluene	0.135	2.12	0.095	1.150		1719	841		851	2192
Alcohol	0.175	2.23	0.085	1.160		2414	894		905	2149
75% alcohol, 25% water	0.227	2.36	0.082	1.156		2818	929		918	2190
50% alcohol, 50% water	0.311	2.43	0.087	1.157		3299	952		973	2200
25% alcohol, 75% water	0.434	2.50	0.107	1.140		3935	991		1025	2216
Water	0.598	2.56	0.141	1.120	1.10	4180	1014	1018	1044	2252